ACR July 1942

NATIONAL ADVISORY COMMITTEE FOR AERONAUTICS

WARTIME REPORT

ORIGINALLY ISSUED
July 1942 as
Advance Confidential Report

PROPELLER SELECTION FROM AERODYNAMIC CONSIDERATIONS

By John L. Crigler and Herbert W. Talkin

Langley Memorial Aeronautical Laboratory
Langley Field, Va.

NACA

WASHINGTON

NATIONAL ADVISORY COMMITTEE FOR AERONAUTICS

ADVANCE CONFIDENTIAL REPORT

PROPELLER SELECTION FROM AERODYNAMIC CONSIDERATIONS

By John L. Crigler and Herbert W. Talkin

SUMMARY

A theoretical analysis is presented of the performance of propellers extending to high values of V/nD. At high values of V/nD the analysis shows the propeller efficiency to be critically dependent on the distribution of the load along the radius. A method of calculating the pitch distributions of optimum propellers is explained. Charts are presented that facilitate the selection of the most efficient propellers over a wide range of operating conditions. It is noted that experimental data in the range of high values of V/nD for the purpose of establishing the optimum load distribution are essentially lacking.

INTRODUCTION

Until recent years the application of propeller theory has been largely restricted to low values of blade angle. Experimental investigations have been made at low values of V/nD or, at best, on propellers designed to operate at low values of V/nD and tested at high values of V/nD. For the low values of V/nD tested, the efficiency depends chiefly on the power absorbed, the speed of advance, and the diameter of the propeller. Other factors of lesser importance are the distribution of thrust along the blade, the number of blades, and the profile drag of the blade sections.

For high-speed airplanes, high values of V/nD are required in order to avoid adverse compressibility effects. Theoretical calculations of propeller efficiencies at high values of V/nD for propellers designed to operate at low values of V/nD agree with the experimental efficiencies obtained. Calculations for the same propellers when the pitch distribution was adjusted to give the Goldstein loading along the blade show materially higher efficiencies and indicate that a major variable for the peak-efficiency condition at high values of V/nD

is the distribution of thrust along the blade.

At airplane speeds of approximately 0.7 the speed of sound, it is necessary to use low lift coefficients in order to avoid compressibility losses, and these low lift coefficients lead to low values of L/D_0 and the profile drag becomes important.

The results of tests of propellers designed for Goldstein loading for each operating condition are reported in reference 1. These tests were made up to a blade angle setting of 43.6° at 0.7 radius, and the efficiency obtained for the operating condition of peak efficiency agrees within 1 percent of that calculated for a Goldstein distribution of loading. This good agreement between the experimental and the theoretical results indicates the possibility of maintaining high efficiencies at high values of V/nD as calculated by using the Goldstein distribution of loading.

The present report shows the values of efficiency that are theoretically possible with a Goldstein load distribution for a wide range of power loadings and values of V/nD for single-rotation propellers of two, three, four, and six blades. It presents a method of determining the pitch distribution to approximate the Goldstein loading for any operating condition. The report is intended to furnish a basis for design of propellers to be tested at high values of V/nD in order to demonstrate the validity of the theoretical analysis in the practical application to aerodynamic design. If the experimental and theoretical analyses are found to agree at high values of V/nD, then theoretical analysis will be available as a reliable basis of aerodynamic design of propellers for any operating condition.

The authors wish to acknowledge the benefit of the unpublished work of Mr. Charles Kaman that was furnished by the Hamilton Standard Propellor Company during the preparation of this report.

SYMBOLS

D propeller diameter

R radius to tip of propeller

r	radius to any blade element
x	radial location of blade element (r/R)
c	chord of blade element
S	disk area of propeller
B	number of propeller blades
α_o	angle of attack of blade element corrected for infinite aspect ratio
β	blade angle setting
ϕ	angle of resultant velocity to plane of rotation $(\beta - \alpha_o)$
ϕ_o	angle of advance of propeller $\left(\tan^{-1} \frac{V}{\pi n D x}\right)$
ϵ	angle of inflow $(\phi - \phi_o)$
n	propeller rotational speed, revolutions per second
σ	propeller element solidity $(Bc/2\pi r)$
V	axial speed of propeller
V_c	speed of sound
ρ	mass density of air
q	dynamic pressure of air stream $(\frac{1}{2} \rho V^2)$
V/nD	advance-diameter ratio of propeller
L	lift of propeller section
D_o	drag of propeller section for infinite aspect ratio
C_L	lift coefficient for infinite aspect ratio
C_D	drag coefficient for infinite aspect ratio
σC_L	propeller element load coefficient
cC_L	blade element load coefficient

γ $\tan^{-1} C_D/C_L$

P input power to propeller

C_P power coefficient $(P/\rho n^3 D^5)$

P_c power disk-loading coefficient (P/qSV)

$\frac{1}{\sqrt{P_c}} = D\sqrt{\frac{\pi\rho V^3}{8P}}$

Q input torque to propeller

C_Q torque coefficient $(Q/\rho n^2 D^5)$

T thrust of propeller

C_T thrust coefficient $(T/\rho n^2 D^4)$

η propeller, or element, efficiency

$\Delta\eta_D$ efficiency loss due to drag $\left\{\frac{V}{\pi nDx}\left[\cot\phi - \cot(\phi+\gamma)\right]\right\}$

$\frac{dC_Q}{dx}$ element torque coefficient $\frac{dQ/dx}{\rho n^2 D^5}$

$\frac{dC_T}{dx}$ element thrust coefficient $\frac{dT/dx}{\rho n^2 D^4}$

a axial-velocity interference factor

a' rotational-velocity interference factor

E_r rotational energy in slipstream

$$\frac{E_r}{P} = \frac{1}{C_Q}\int_{0.2}^{1.0} a' \frac{dC_Q}{dx}\,dx$$

F tip-loss coefficient

FORMULAS

The formulas employed for making the propeller-blade-element calculations in this report are taken from reference 2. From this reference are obtained the relations

$$\frac{a'}{1 - a'} = \frac{\sigma(C_L \sin \phi + C_D \cos \phi)}{4F \sin \phi \cos \phi} \tag{1}$$

and

$$\frac{a}{1 + a} = \frac{\sigma(C_L \cos \phi - C_D \sin \phi)}{4F \sin^2 \phi} \tag{2}$$

It appears that the drag terms should be omitted from these equations because the retarded air due to drag is restricted to thin helical sheets in the wake and can have no appreciable effect on the general inflow factors a and a'. These equations then become

$$\frac{a'}{1 - a'} = \frac{\sigma C_L}{4F \cos \phi} \tag{3}$$

and

$$\frac{a}{1 + a} = \frac{\sigma C_L \cot \phi}{4F \sin \phi} \tag{4}$$

With these equations an expression for the blade element loading may be obtained:

$$\frac{\sigma C_L}{F} = \frac{4 \sin \epsilon \left(1 + \frac{\pi n D x}{V} \tan \epsilon\right)}{\sqrt{\left(\frac{\pi n D x}{V}\right)^2 + 1}} \tag{5}$$

For small values of ϵ this equation becomes

$$\frac{\sigma C_L}{F} \approx \frac{4\epsilon \left(1 + \frac{\pi n D x}{V} \epsilon\right)}{\sqrt{\left(\frac{\pi n D x}{V}\right)^2 + 1}} \tag{6}$$

This formula was used in constructing figure 1. The solution of equation (6) for ϵ is

$$\epsilon = \frac{1}{2\,\frac{\pi nDx}{V}}\left(\sqrt{1 + \frac{\frac{\pi nDx}{V}\,\sigma C_L}{F}\sqrt{\left(\frac{\pi nDx}{V}\right)^2 + 1}} - 1\right) \qquad (7)$$

Formula (7) is useful for solutions outside the scope of the chart.

The expression for the element efficiency is

$$\eta = \frac{V}{\pi nDx}\cot(\phi + \gamma) \qquad (8)$$

The element efficiency without friction is obtained from this formula, omitting γ. The efficiency loss $\Delta\eta_D$ due to friction drag is then given by the difference between these two expressions for η:

$$\Delta\eta_D = \frac{V}{\pi nDx}\left[\cot\phi - \cot(\phi + \gamma)\right] \qquad (9)$$

The expression for the rotational-energy loss is derived in reference 3.

$$\frac{E_r}{P} = \frac{1}{C_Q}\int_0^1 a'\,\frac{dC_Q}{dx}\,dx \qquad (10)$$

RESULTS

Figure 2 gives the tip-loss factor F as used in this report for two-, three-, four-, and six-blade propellers. Reference 4 gives the corrections for two-, three-, and four-blade propellers and a method of extrapolation to obtain the corrections for use with a six-blade propeller. The data of reference 4 were extrapolated to $x = 0.2$ for the two-, three-, and four-blade propellers.

Figure 3 shows the ratio of the element load coefficient cC_L to the load coefficient at the 0.7 radius for two-, three-, four-, and six-blade propellers having the Goldstein distribution operating at values of V/nD from 1.0 to 5.0. The method used in obtaining the distribution of the element load coefficient is outlined by Bairstow in reference 5. For constant C_L along the radius, the curves give the plan form for maximum efficiency at a given value of V/nD. Any departure from this plan form may be made without any sacrifice in efficiency provided that C_L is adjusted to keep cC_L as shown on the figure, except for losses due to changes in L/D_0 of the sections.

For operation at low values of V/nD and torque coefficient, the chief losses in efficiency arise from the axial motion imparted to the slipstream and the blade drag. At

high values of V/nD and torque coefficient, however, the percentage power loss in axial momentum is very small and the loss in efficiency due to the rotational velocity becomes important. The rotational-energy loss is proportional to a', which in turn is inversely proportional to x^3 (reference 3), so that a large portion of the energy losses may arise from this source over the inner radii. For this reason it would be desirable to unload the inner sections of the blade as V/nD increases. On the other hand, the Goldstein tip-loss correction at a given radius increases with increasing ϕ or V/nD, which results in greater loss of efficiency at the tips of the blades. The two effects, which are a function of V/nD, tend to move the location of the maximum element loading in opposite directions. The first effect predominates, however, and it may be seen in figure 3 that the loading should be more concentrated toward the tip with increasing V/nD, although for values of V/nD of 3 or more, there is seen to be little change in optimum load distribution.

Figure 4 shows the radial location of the maximum value of the element load coefficient cC_L against V/nD for optimum load distribution for two-, three-, four-, and six-blade propellers. It is seen that the maximum value of cC_L should move toward the propeller tip with an increase in the number of blades because tip loss approaches zero for an infinite number of blades. The curves also show that the maximum value of cC_L should move toward the propeller tip with an increase in operating V/nD.

The loss of element efficiency due to drag, $\Delta\eta_D$, is plotted against V/nDx in figure 5, as calculated by equation (9) for a wide range of values of L/D_0. Values of C_L for a 9-percent Clark Y section taken from figure 10 are shown on the curves of L/D_0. The total loss in efficiency resulting from the profile drag of the blade is seen to be only a little more than 3 percent for elements operating at the usual present-day value of C_L of roughly 0.45, corresponding to an L/D_0 of 60, in the range of V/nDx from 2.0 to 5.0. For the same L/D_0 at higher values of V/nDx, this loss is increased, for example, to 11 percent at the value of V/nDx = 20. The efficiency loss due to profile drag becomes important also at the lower values of L/D_0. Low values of L/D_0 may arise from the use of small lift coefficients in an effort to increase the section speed at which compressibility shock is encountered. If a C_L of 0.25 is used, for example, on a blade section operating at a V/nDx of 7.5, the friction loss will be more than 7 percent (L/D_0 = 38). This value represents the loss at a V/nD of 5.25 for the 0.7 radius. At x = 0.3 and V/nD = 5.25, V/nDx is 17.5 and the loss is 15 percent for an L/D_0 = 38.

A value of $L/D_0 = 38$ is unattainable for the thick inner sections at the condition of optimum distribution for $V/nD = 5.25$ and $C_L = 0.25$ at the 0.7 radius. For this reason the loss in element efficiency will be greater than 15 percent at $x = 0.03$ for the specified conditions but since only a small proportion of power is absorbed on these sections, the effect on the total efficiency will be small. This effect may be seen in figure 6, which shows the optimum distribution along the radius of the ratio of the element torque coefficient to the element torque coefficient at the 0.7 radius for three values of V/nD for a three-blade propeller with constant L/D_0 along the radius.

The basic propeller selection charts of this report are presented in figure 7. The curves have been drawn through points obtained from optimum torque and thrust distributions graphically integrated from the tip of the blade to $x = 0.2$. The ordinates give values of efficiency for propellers with blade sections operating at $L/D_0 = 60$. The abscissas represent values of $\frac{1}{\sqrt{P_c}} = D\sqrt{\frac{\pi\rho V^3}{8P}}$, so that this scale is linear in propeller diameter. Against these scales are shown, in solid lines, curves of constant propeller element load coefficient σC_L at 0.7R over a wide range of values for two-, three-, four-, and six-blade propellers having optimum load distributions. These curves are crossed by families of dashed curves of constant advance-diameter ratio V/nD for values of V/nD from 1.0 to 5.0.

The dotted curves of σC_L represent a nominal value of σC_L that is in the normal range as used on conventional propellers. These curves are included as a means of orientation and are plotted together for two-, three-, four-, and six-blade propellers in figure 8. This chart is useful to obtain a first approximation to the required number of conventional blades. It should be noted that figures 7 and 8 apply strictly only to propeller blades, all the elements of which operate at the same value of $L/D_0 = 60$. The usefulness of these figures can be extended, at least qualitatively, to other values of L/D_0 for the entire blade or for various radial elements of the blade by means of figure 5. It may also be seen in figure 7 that, for a fixed value of P_c, a gain in efficiency may be realized by operating at a decreased value of cC_L

and lower values of V/nD. Thus, for any propeller installation, it is advantageous to operate the propeller at the lowest value of V/nD possible and still avoid compressibility losses. The lower values of V/nD are not attainable in modern designs for high-speed flight, however, because of aerodynamic limitations on section speed.

For a given power and flight speed and for constant tip speed, the increase in efficiency with diameter for corresponding decreases in solidity may be followed directly on a curve of constant V/nD in figure 7. Following along a given V/nD curve, the efficiency can be continuously increased until a practical limitation on the minimum value of σC_L or the maximum diameter is reached.

In figure 9, values of η at $V/nD = 2.5$ have been plotted against σC_L at 0.7R for two-, three-, four-, and six-blade propellers. This figure affords a means of estimating the decrease in η with increasing σC_L obtained by increasing the number of blades in one case or by increasing the blade width in the other. The figure also shows the gain in efficiency to be expected for a given solidity from increasing the number of blades. These curves are crossed by a dotted standard curve of constant width per blade. The dotted curve shows the change in efficiency to be expected from tests on propellers of two, three, four, and six blades of constant width per blade.

DISCUSSION

Conventional plan forms are generally relatively too wide along the inner radii for the high values of V/nD needed for present-day applications. A typical chord distribution of Bureau of Aeronautics propeller 5868-9 is shown in figure 3(a). It may be seen that, if C_L is constant along the radius, the chord distribution will closely approximate the optimum for a two-blade propeller for operation at a V/nD of slightly less than 2.5, whereas some present-day applications may require a V/nD of 5.0 or more.

The effect on the propeller efficiency of using a fixed chord distribution and varying the value of C_L to obtain the optimum distribution of σC_L for the desired operating condition was estimated as follows:

The optimum blade plan form with constant C_L for a three-blade propeller at $V/nD = 1.0$ was used for computing its performance at $V/nD = 5.0$ with the distribution of the element load coefficient σC_L adjusted to give the optimum distribution of cC_L at $V/nD = 5.0$ by varying only C_L.

For illustrative purposes Clark Y 12-percent sections have been assumed. The data for these sections were taken from reference 6 and are plotted in figure 10. Curves of C_L for constant angle of attack are plotted against thickness ratio in the lower part of the figure. The thickness ratio is the ratio of the maximum thickness of the blade element to its chord. In the upper part are plotted curves of L/D_0 for constant C_L against thickness ratio. The distributions of cC_L for the propeller are shown in figure 3 and the design calculations are given in table I. The changes in element efficiency are the direct result of changes in L/D_0 corresponding to C_L. The result will be influenced somewhat by the relation of the element C_L to the C_L for maximum L/D_0.

In the illustration both blades have the same value of σC_L at $x = 0.7$ and all sections operate below C_L for maximum L/D_0. It will be noted that L/D_0 increased slightly from $x = 0.7$ to the tip of the blade but fell rapidly over the inner sections from 60 at $x = 0.7$ to 21 at $x = 0.2$. The propeller efficiency is 0.860 as compared with 0.871 obtained with optimum chord distribution (fig. 7). The loss in efficiency as a result of using the plan form of blade 5868-9 instead of the optimum, therefore, may not be expected to be much greater than 1 percent of the power. The thick sections near the hub, however, will produce an additional loss.

A much more serious loss in efficiency results from the common practice of adapting a blade designed for low values of V/nD to operate at higher values by simply turning the blade in the hub. In order to illustrate this case, the optimum blade for $V/nD = 1.0$ for a three-blade propeller was analyzed for operation at $V/nD = 5.0$ by adding a constant angle to β for all elements, the total power coefficient being adjusted to about the same value as for the optimum propeller at $V/nD = 5.0$. By this procedure the efficiency obtained is 0.765 as compared with 0.871 for the optimum propeller at $V/nD = 5.0$. The calculations are shown in table II. Over most of the blade the

value of L/D_o has fallen from 60 to around 45, and this result accounts for a small part of the efficiency loss. (Cf. fig. 5.) The greatest portion of the loss, however, is the increase of rotational energy in the slipstream resulting from overloading the inner portion of the blade. The torque distributions for the two propellers are shown in figure 11. The rotational-energy losses are compared in figure 12 as computed by the method described in reference 3. These losses are seen to be 4.5 percent and 14.2 percent for the optimum and the twisted blades, respectively.

Computations of the foregoing type have been used to analyze the performance obtained in tests of propellers designed for low values of V/nD and tested at high values of V/nD. The close agreement between computations and test results has led to the conclusion that the most important variable for operation at high values of V/nD is the pitch distribution of the propeller. Tests of propellers of optimum pitch distribution at high values of V/nD are urgently needed.

PROPELLER SELECTION

For a given airplane-engine unit, the quantity $\sqrt{\frac{\pi\rho V^3}{8P}}$ will, in general, be fixed at a known value. There remain to be determined the number of blades B, the propeller element loading coefficient σC_L, the rotative speed n, and the propeller diameter D. The effects on the efficiency of changes in these four variables can be readily followed on the selection charts (figs. 7 and 8).

Several examples are given here to demonstrate the use of the design charts (fig. 7) in determining the proper relation between all the variables in the selection of a propeller for any given set of conditions. In the examples it is assumed that tests are available giving the critical Mach number for the propeller sections for contemplated use. Tests to obtain these data are urgently needed as existing data of this nature are scant and unreliable.

Example I

It is assumed, for the purposes of illustration, that all the propeller sections are known to be free from undue compressibility losses if standard blades are used, if the lift coefficient does not exceed 0.55 at 0.7 radius, and if the propeller tip speed does not exceed 80 percent of the speed of sound. The design conditions are as follows:

Power, horsepower	2,000
Altitude, feet	25,000
Velocity, miles per hour	400
Tip speed, $(0.80\ V_c)$, feet per second	811
$\pi nD = \sqrt{(\text{tip speed})^2 - V^2}$, feet per second	559
V/nD	3.30
$\sqrt{\frac{\pi\rho V^3}{8P}}$	0.2772

	Four blades	Six blades
$D\sqrt{\frac{\pi\rho V^3}{8P}}$	4.75	3.90
D, feet	17.15	14.05
Estimated weight, pounds	1030	870
Propeller rotational speed, rpm	623	760

In example I it was assumed that the propeller drive gear ratio was optional. The results show that, if a standard four-blade propeller is used, a diameter of 17.15 feet will be required but that a diameter of only 14.05 feet is required if a six-blade propeller is used.

The preceding process may be repeated with other tip speeds provided that the corrections for compressibility are known. The selection of the proper tip speed for a given application requires the use of experimental data that are not available for an accurate solution.

It is now necessary to go to figure 3 to obtain the proper distribution of cC_L along the radius for a value of $V/nD = 3.30$. The desired propeller blade angle for any radius may be obtained by successive approximations as follows:

From ϕ_o and x an approximation to F is made, which is used in calculating $\frac{BcC_L}{2\pi rF}$.

Then the first approximation to ϵ^o is made where

$$\epsilon^o = 28.65 \left[\sqrt{\left(\frac{V}{\pi nDx}\right)^2 + \frac{\sigma C_L}{F}\sqrt{1 + \left(\frac{V}{\pi nDx}\right)^2}} - \frac{V}{\pi nDx} \right]$$

For convenience, ϵ^o has been plotted against $\frac{BcC_L}{2\pi rF}$ for a wide range of values of $\frac{nDx}{V}$ in figure 1.

A first approximation to ϕ is now obtained, $\phi = (\phi_o + \epsilon)$. With this value of ϕ and x, a new F is obtained and the process is repeated to obtain the second approximation to ϕ. Usually, two successive approximations give ϕ to the desired degree of accuracy. Then with C_L and the airfoil section known, α_o may be obtained from airfoil data corrected to infinite aspect ratio. The blade angle setting $\beta = \phi + \alpha_o$.

This process may be carried out for as many section radii as desired.

If a propeller designed for optimum distribution in free air is operated on the axis of a body, such as an open-nose cowling, the portions of the blade in the regions of reduced velocity will experience an increased lift coefficient with the result that the load distribution will no longer be optimum. The blade will be locally overloaded and may even stall. The region of reduced axial velocity occurs almost invariably over the blade sections near the hub, so that the overloading in this region will result in large rotational-energy losses. In such cases, designing for the local velocity distribution is therefore imperative. Calculations indicate that a close approximation to the optimum distribution in such cases will be obtained by adjusting the blade angle of the blade to obtain the distribution of cC_L appropriate to a propeller in the free stream operating at the V/nD of the tip.

Example II

In some cases the maximum allowable diameter as well as the selection of gear ratio, and thus the propeller speed to be used, will be specified. It is proposed to select a propeller thus limited for the engine power, altitude, and forward velocity given in example I. The limitations on the propeller and the design are as follows:

Propeller diameter, feet	12.8
Propeller speed, rpm	1200
$\frac{1}{\sqrt{P_c}} = D\sqrt{\frac{\pi\rho V^3}{8P}}$	3.55
V/nD	2.29
σC_L at 0.7R (fig. 7(c))	0.0733
Tip speed = $\sqrt{(\pi nD)^2 + V^2}$, feet per second . . .	1000

The computations show that a standard four-blade propeller operating with a lift coefficient of 0.55 at the 0.7 radius will absorb the engine power (if no losses are incurred because of compressibility), but the propeller tip translational velocity will be 98.5 percent the velocity of sound. This tip speed is undoubtedly too high to avoid some compressibility losses over at least the outer portion of the blade.

If the tip portions of the blade were cut off in an attempt to reduce the tip speed, it would be necessary to use higher lift coefficients over the rest of the blade to absorb the power, thus lowering the critical Mach number of the sections. The propeller efficiency would also tend to decrease as a result of the reduction in diameter. The best compromise obtainable by cutting off the propeller tip is thus seen to be critically dependent on the variation of section critical Mach number with lift coefficient, but it is unlikely that, in a given case, much improvement in propeller efficiency may be achieved by this procedure.

Example III

Compressibility losses on a propeller for constant power will be comparatively insensitive to changes over a wide range of rotative speed. Thus, if a propeller section is operating near its critical Mach number and the rotative speed is increased at the same value of P_c, the Mach number will increase accordingly. Also, the value of C_L required for the section will decrease and this result will raise the critical Mach number. An example illustrating a typical case is here given.

Design conditions:

Engine power, horsepower	2,000
Altitude, feet	25,000
Velocity, miles per hour	400
Propeller diameter, feet	13.17
Number of blades	6
$\frac{1}{\sqrt{P_c}} = D\sqrt{\frac{\pi\rho V^3}{8P}}$	3.65

	First choice	Second choice
Rotational speed, rpm	1080	900
V/nD	2.48	2.97
Tip speed, feet per second	948	854
fraction of V_c	0.934	0.842
Speed at 0.7R, feet per second	785	730
fraction of V_c	0.773	0.719
$\sigma . C_L$ at 0.7 radius	0.0800	0.1070
C_L at 0.7 radius	0.400	0.535

Calculations are shown for two rotative speeds, 1080 and 900 rpm. The blade section translation speeds at $x = 0.7$ are seen to have the translation Mach numbers 0.773 and 0.719, respectively, while the required section C_L is raised from 0.400 to 0.535; thus the increase in C_L tends to compensate for the decrease in translational Mach number.

Langley Memorial Aeronautical Laboratory,
National Advisory Committee for Aeronautics,
Langley Field, Va.

REFERENCES

1. Lock, C. N. H., and Bateman, H.: Wind Tunnel Tests of High Pitch Airscrews. Part II. Variations of Blade Width and Blade Section. R. & M. No. 1729, British A.R.C., 1936.

2. Glauert, H.: Airplane Propellers. Vol. IV, div. L of Aerodynamic Theory, W. F. Durand, ed., Julius Springer (Berlin), 1935, pp. 169-360.

3. Stickle, George W., and Crigler, John L.: Propeller Analysis from Experimental Data. Rep. No. 712, NACA, 1941.

4. Lock, C. N. H., and Yeatman, D.: Tables for Use in an Improved Method of Airscrew Strip Theory Calculation. R. & M. No. 1674, British A.R.C., 1935.

5. Bairstow, Leonard: Applied Aerodynamics. Longmans, Green and Co., 2d ed., 1939, p. 642.

6. Pinkerton, Robert M., and Greenberg, Harry: Aerodynamic Characteristics of a Large Number of Airfoils Tested in the Variable-Density Wind Tunnel. Rep. No. 628, NACA, 1938.

TABLE I

BLADE WITH OPTIMUM CHORD DISTRIBUTION FOR THREE-BLADE PROPELLER AT $V/nD = 1.0$
ADJUSTED TO OPTIMUM DISTRIBUTION OF σC_L FOR $V/nD = 5.0$

$[\eta = 0.860; \quad C_Q = 0.1593]$

x	$B\frac{c}{r}$	ϕ_o (deg)	ϕ (deg)	F	C_L	α_o (deg)	L/D_o	η	c/R	$\frac{dC_Q}{dx}$	$\frac{dC_T}{dx}$
0.20	2.310	82.84	83.46	1.479	0.173	-3.6	21	0.527	0.154	0.0254	0.0169
.30	1.820	79.33	80.20	1.148	.236	-3.0	28	.726	.182	.0627	.0572
.45	1.285	74.21	75.48	.827	.346	-1.9	41	.825	.193	.1481	.1535
.60	.845	69.34	70.90	.607	.470	-.6	54	.864	.169	.2389	.2594
.70	.628	66.26	68.03	.483	.550	.2	60	.874	.147	.2965	.3255
.80	.469	63.31	65.31	.365	.619	.9	65	.878	.125	.3325	.3667
.90	.280	60.51	62.56	.241	.681	1.5	68	.885	.084	.2866	.3189
.95	.185	59.18	61.25	.168	.720	1.9	70	.888	.059	.2271	.2535

TABLE II

BLADE WITH OPTIMUM CHORD DISTRIBUTION FOR THREE-BLADE PROPELLER AT $V/nD = 1.0$
TURNED IN HUB TO OPERATE AT $V/nD = 5.0$

$[\eta = 0.765; \quad C_Q = 0.1661]$

x	$B\frac{c}{r}$	ϕ_o (deg)	ϕ (deg)	F	C_L	α_o (deg)	L/D_o	η	c/R	$\frac{dC_Q}{dx}$	$\frac{dC_T}{dx}$
0.20	2.310	82.84	88.04	1.508	1.480	11.80	46	0.099	0.154	0.2170	0.0269
.30	1.820	79.33	83.13	1.160	1.050	5.35	70	.562	.182	.2792	.1974
.45	1.285	74.21	76.39	.827	.598	.65	65	.799	.193	.2553	.2564
.60	.845	69.34	70.69	.607	.400	-1.35	47	.867	.169	.2058	.2242
.70	.628	66.26	67.40	.485	.350	-1.80	42	.884	.147	.1897	.2107
.80	.469	63.31	64.44	.367	.350	-1.80	42	.894	.125	.1867	.2098
.90	.280	60.51	61.66	.243	.382	-1.55	45	.903	.084	.1594	.1811
.95	.185	59.18	60.37	.170	.410	-1.20	48	.907	.059	.1300	.1482

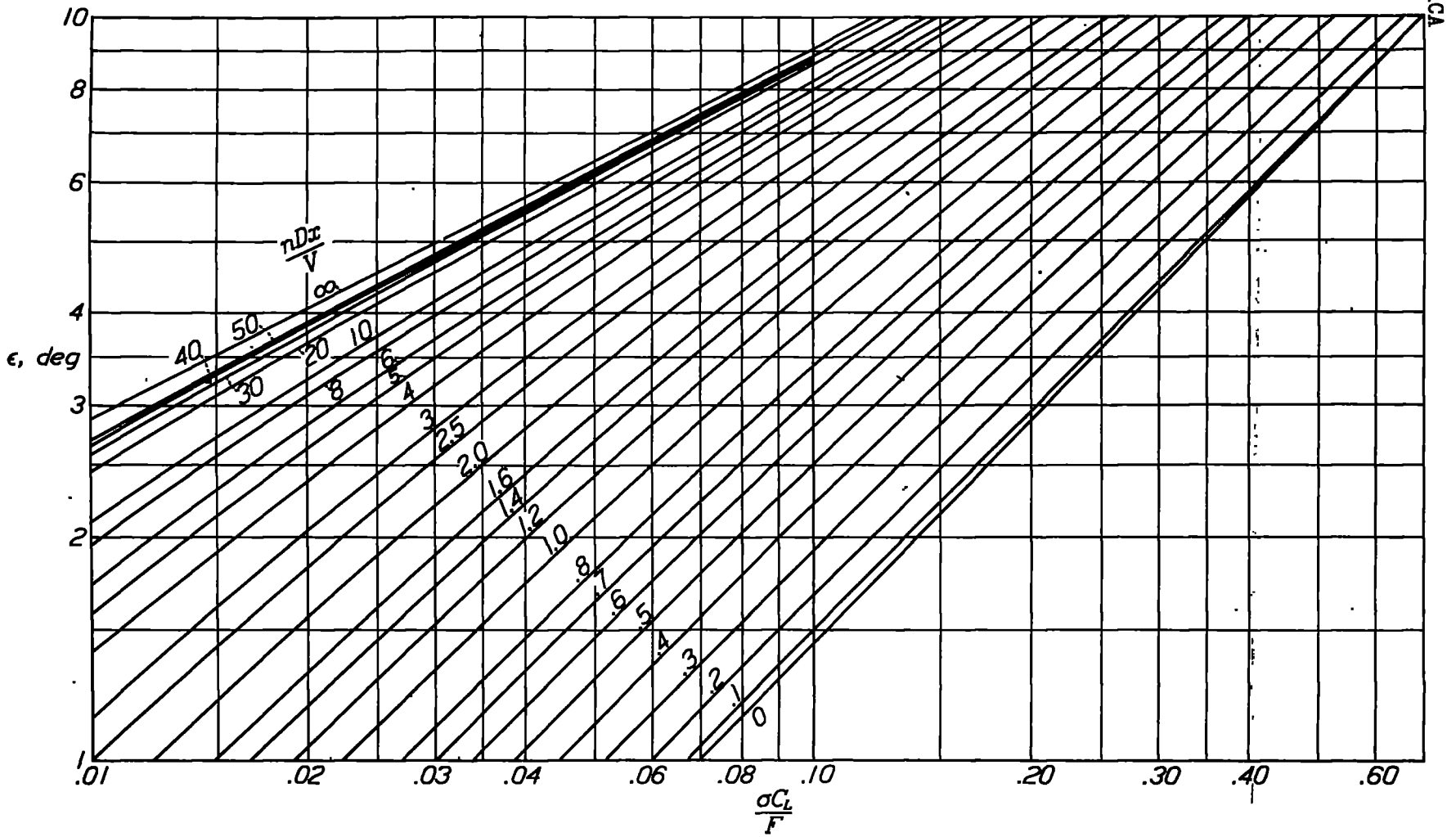

Figure 1.- Chart of ε against $\frac{\sigma C_L}{F}$ for values of $\frac{nD_x}{V}$ from 0 to ∞.

$\frac{nD_x}{V} = \frac{79.2 \times 1.97 \times .7}{80} = .4365$

$\epsilon \sim 5.8°$ calculated to $6.2°$

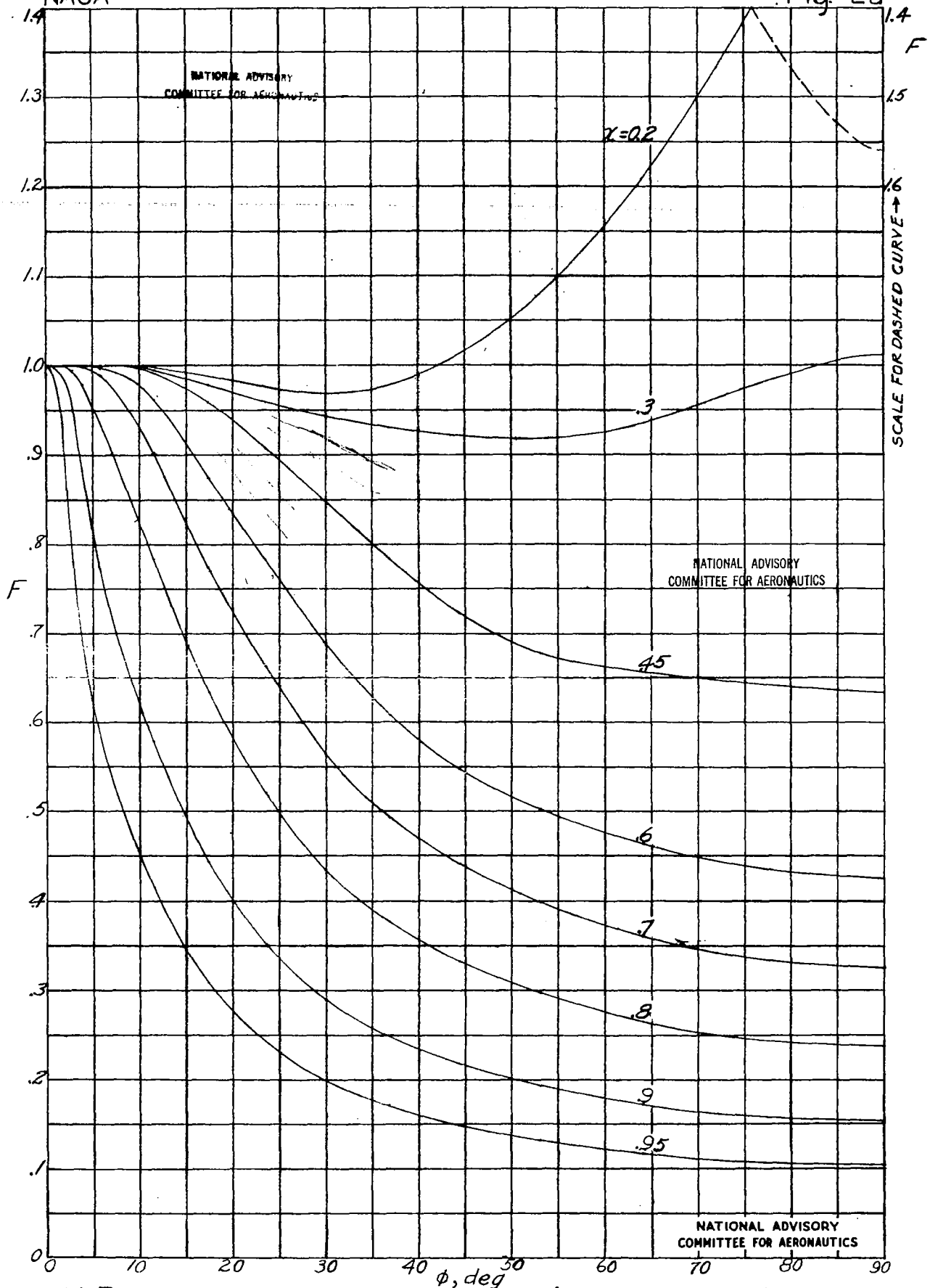

(a) For two-blade propellers. (Data from reference 4.)

Figure 2.- Curves of F against φ.

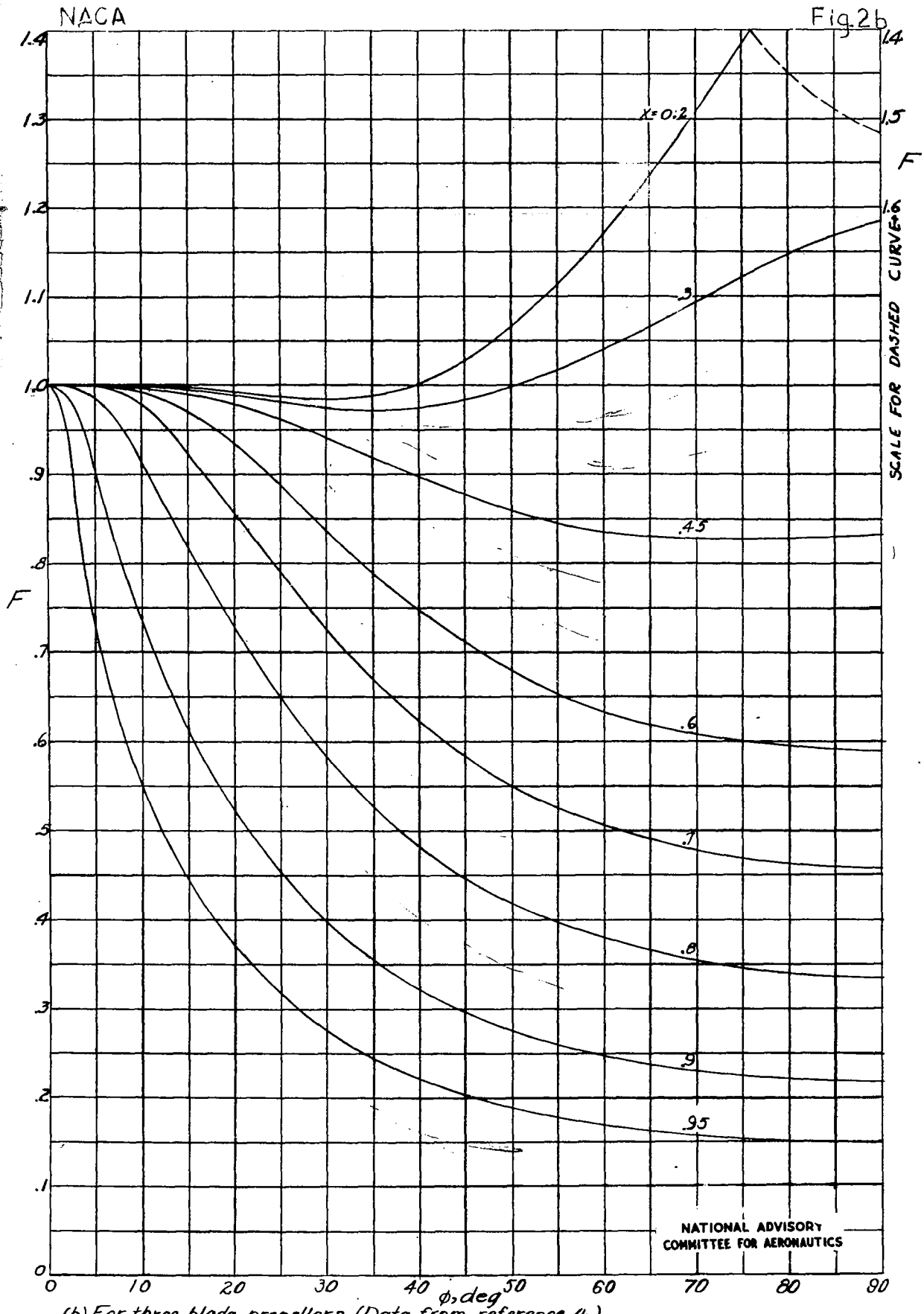

(b) For three-blade propellers. (Data from reference 4.)

Figure 2 — Continued.

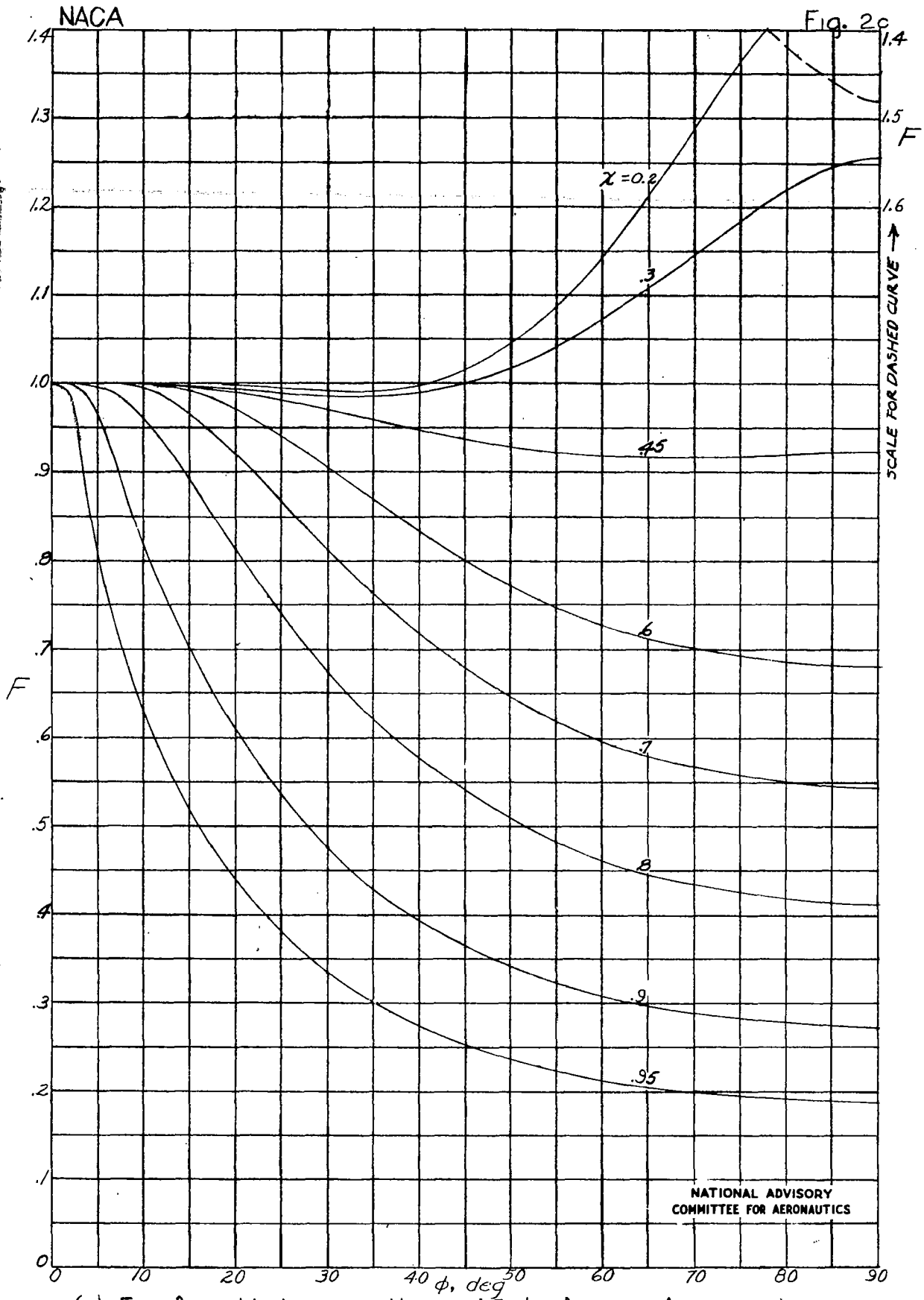

(c) For four-blade propellers. (Data from reference 4.)

Figure 2. - Continued.

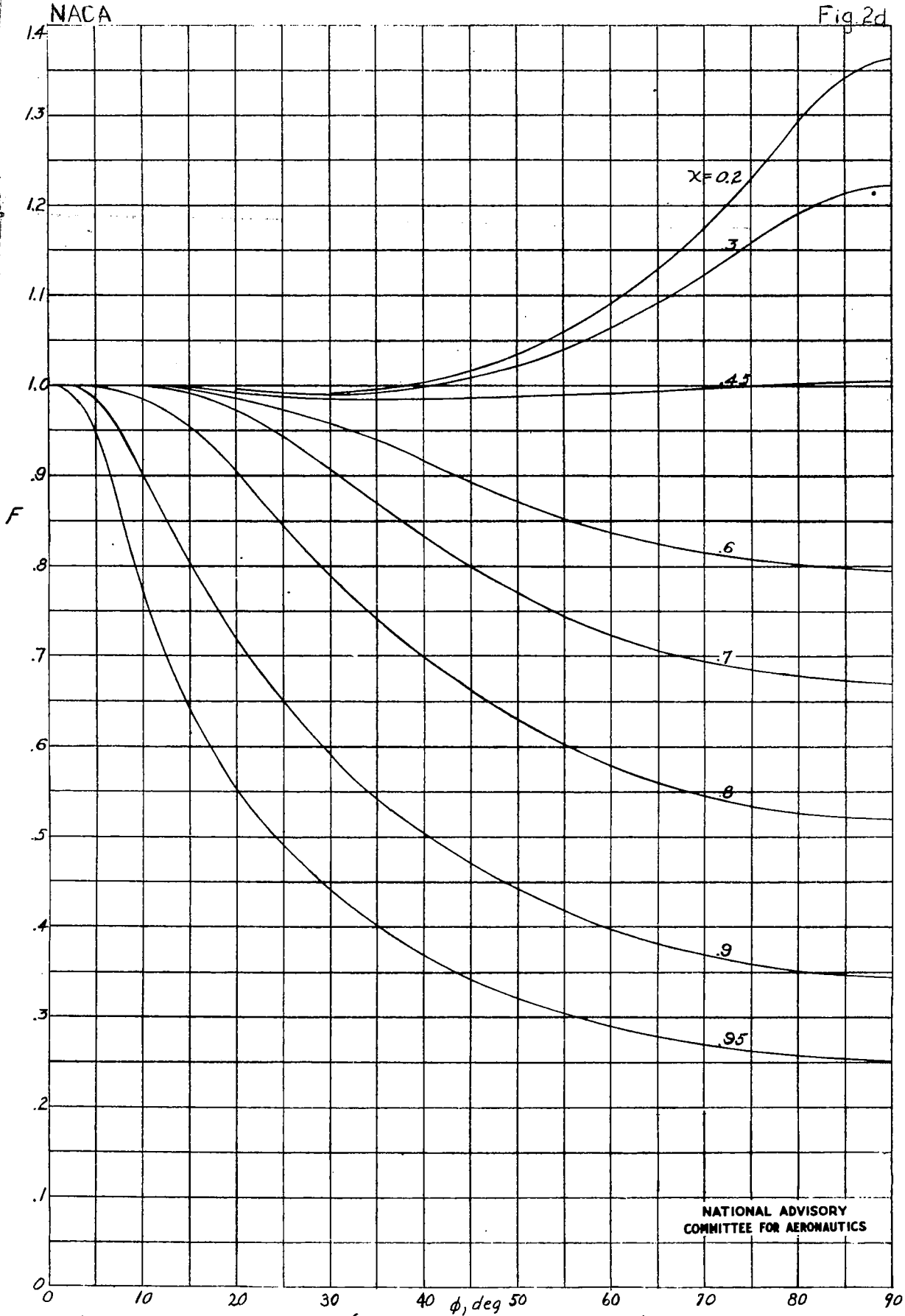

(d) For six-blade propellers. (Extrapolated from reference 4.)

Figure 2.- Concluded.

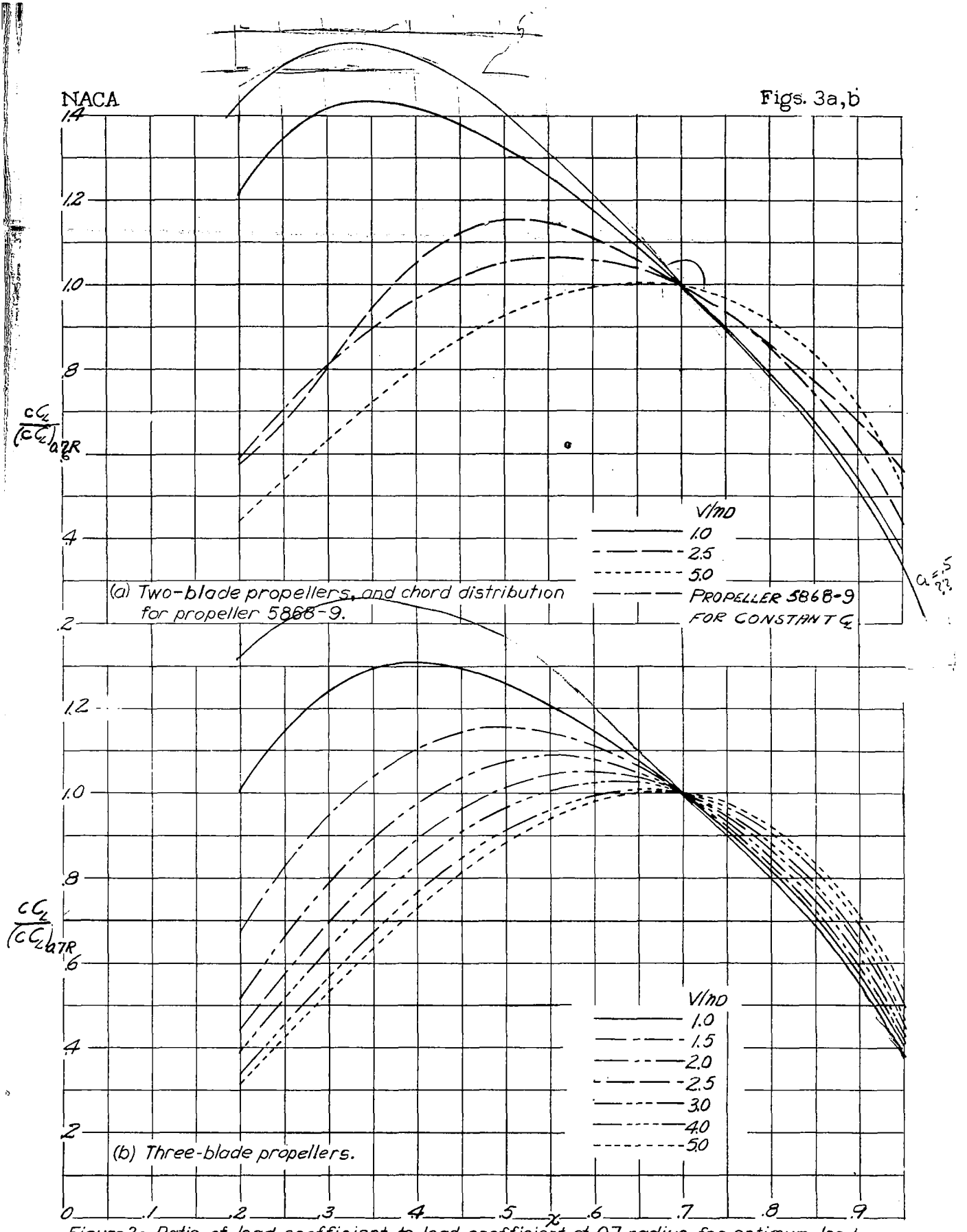

Figure 3.- Ratio of load coefficient to load coefficient at 0.7 radius for optimum load distribution for propellers operating at several values of V/nD (a to d)

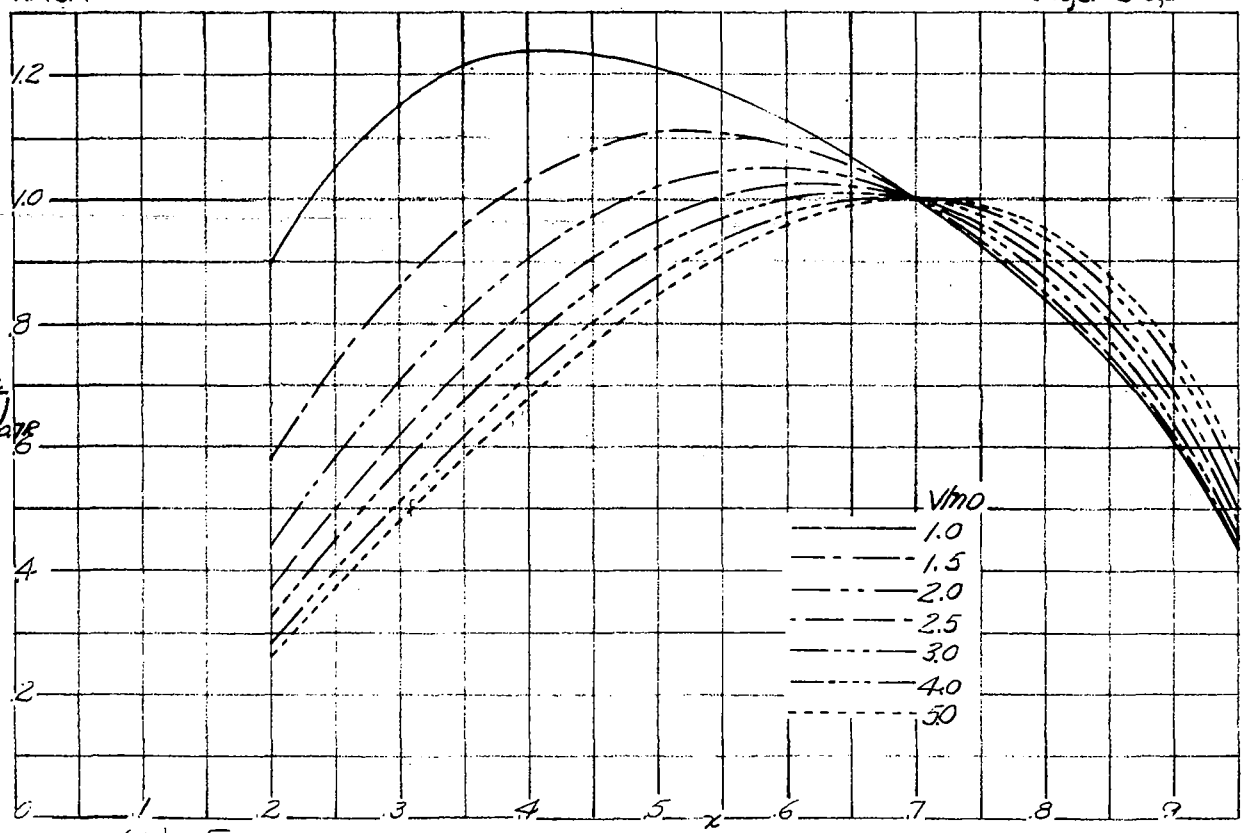

(C) FOUR-BLADE PROPELLERS.

FIGURE 3.- CONTINUED

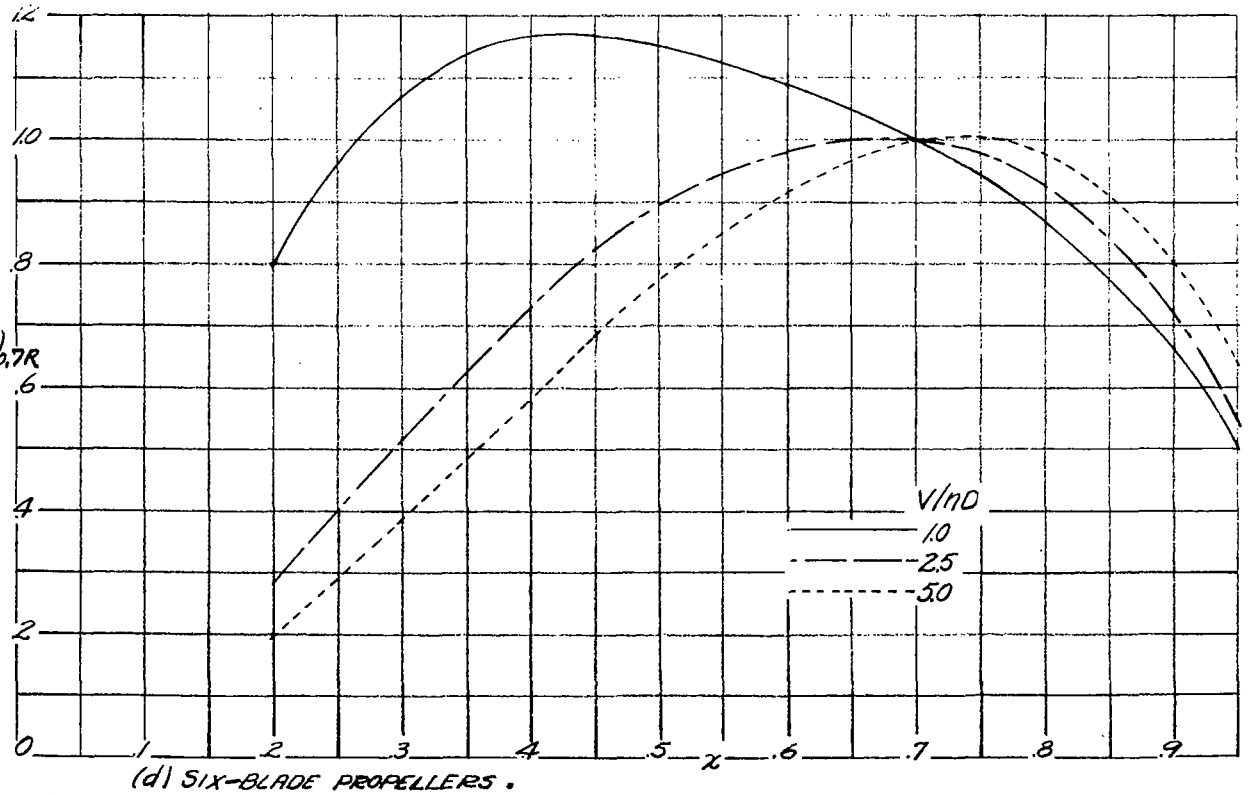

(d) SIX-BLADE PROPELLERS.

FIGURE 3.- CONCLUDED.

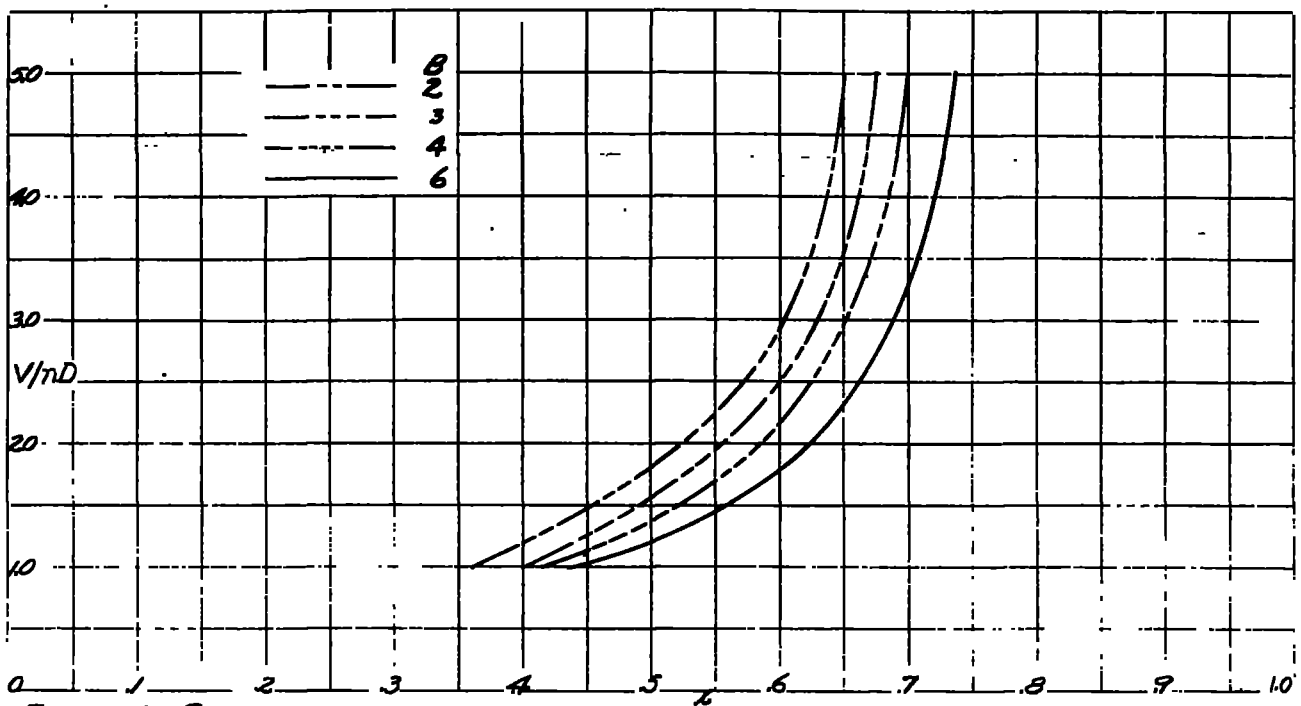

FIGURE 4.- CURVE SHOWING RADIAL LOCATION OF MAXIMUM VALUE OF ELEMENT LOAD COEFFICIENT c_{C_L} FOR OPTIMUM THRUST DISTRIBUTION [illegible] V/nD.

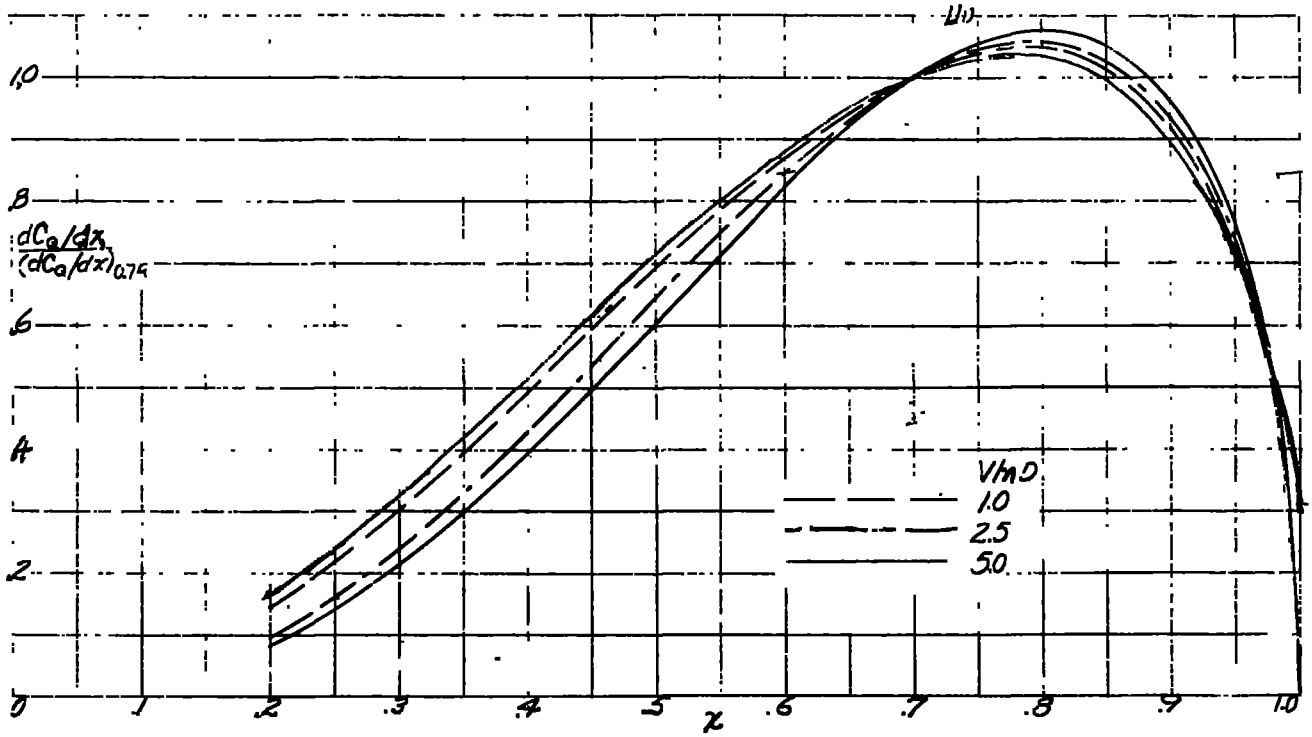

FIGURE 6.- RATIO OF dC_a/dx TO dC_a/dx AT 0.7 RADIUS FOR SEVERAL VALUES OF V/nD FOR A THREE-BLADE PROPELLER.

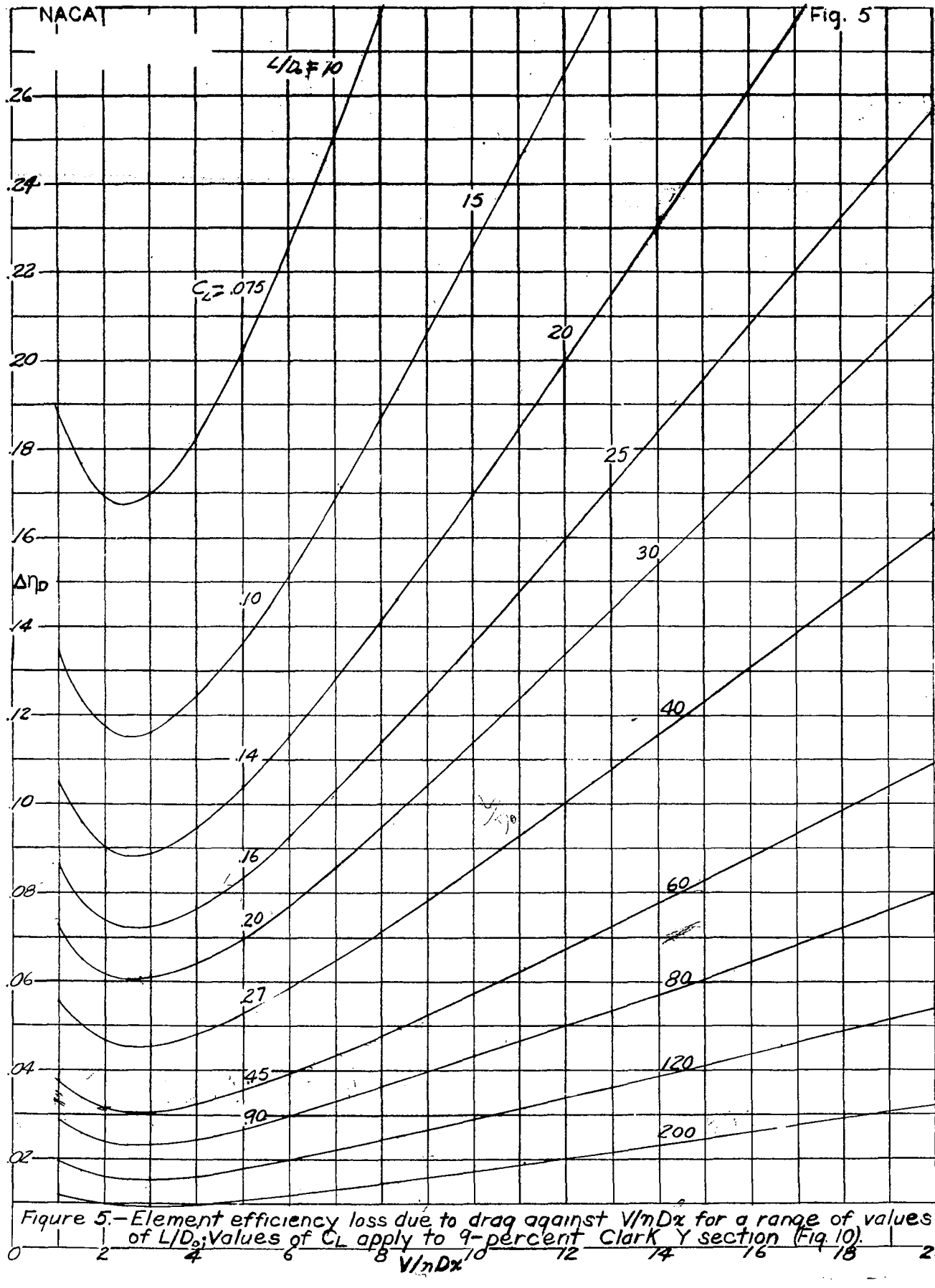

Figure 5.—Element efficiency loss due to drag against V/nDx for a range of values of L/D_o; Values of C_L apply to 9-percent Clark Y section (Fig. 10).

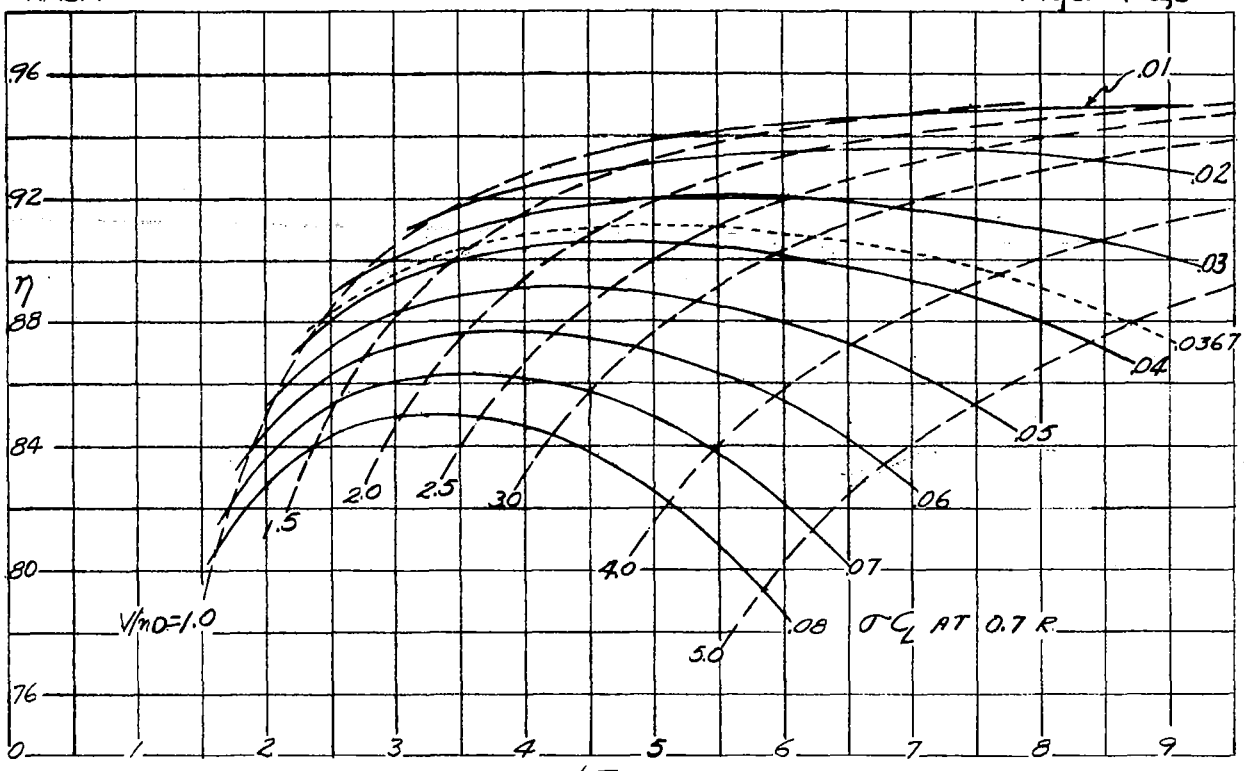

(a) TWO-BLADE PROPELLERS.

FIGURE 7(a to d).- PROPELLER DESIGN CHART. ELEMENT L/D₀=60.

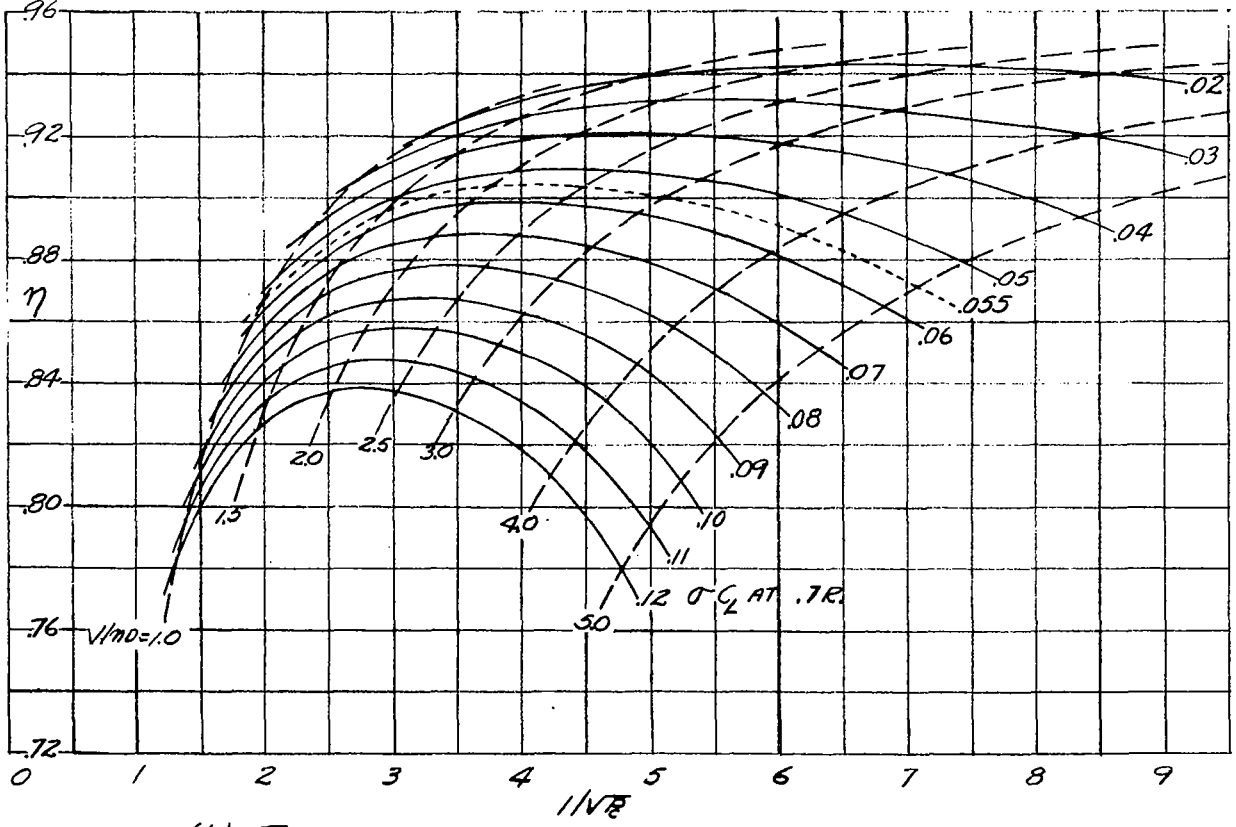

(b) THREE-BLADE PROPELLERS.

FIGURE 7.- CONTINUED.

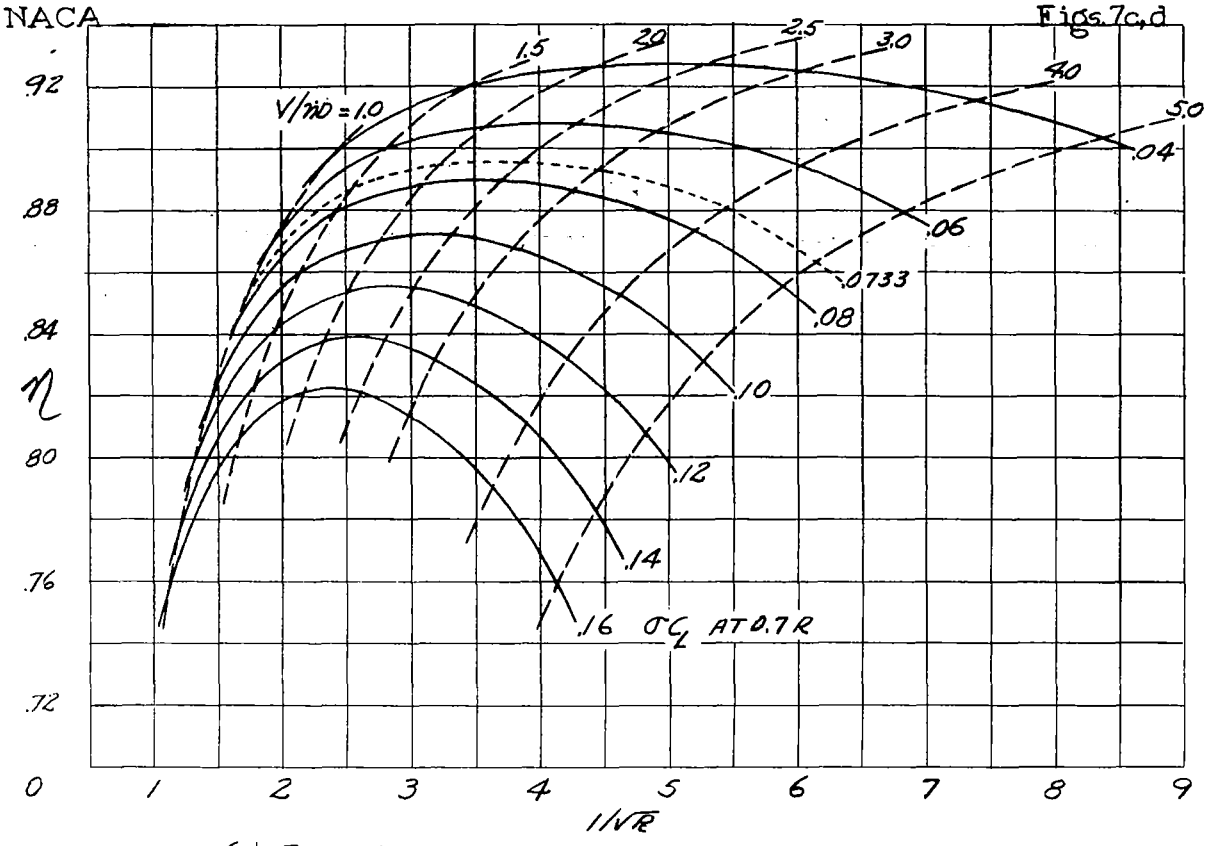

(c) FOUR-BLADE PROPELLERS.

FIGURE 7.- CONTINUED.

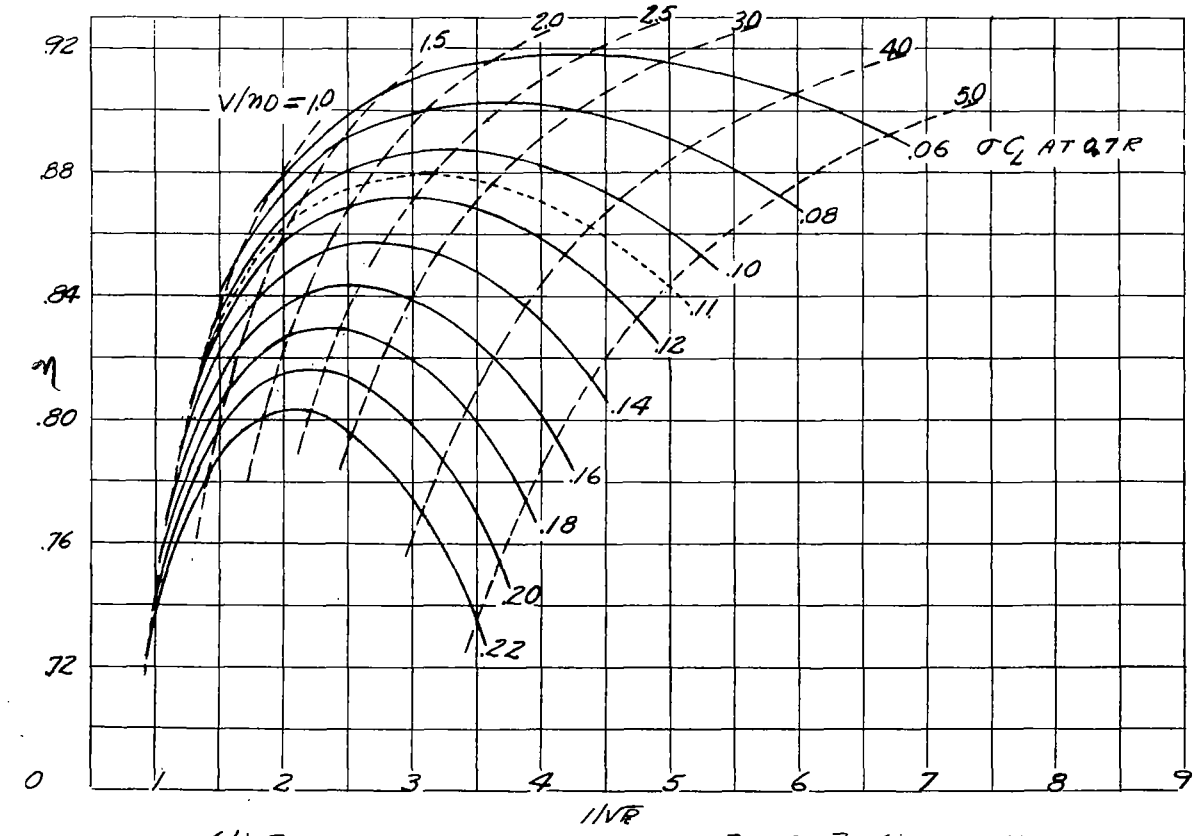

(d) SIX-BLADE PROPELLERS.

FIGURE 7.- CONCLUDED

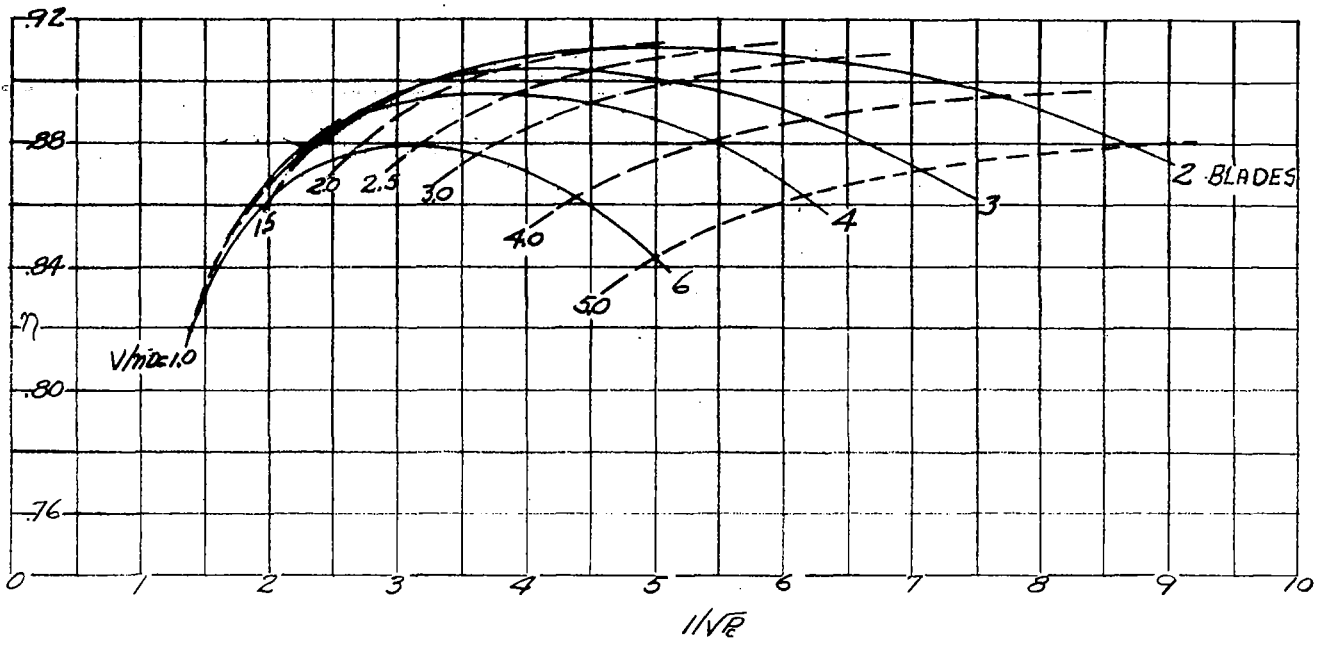

FIGURE 8.—DESIGN CHART FOR STANDARD PROPELLER BLADES. ELEMENT $4/D_0 = 60$.

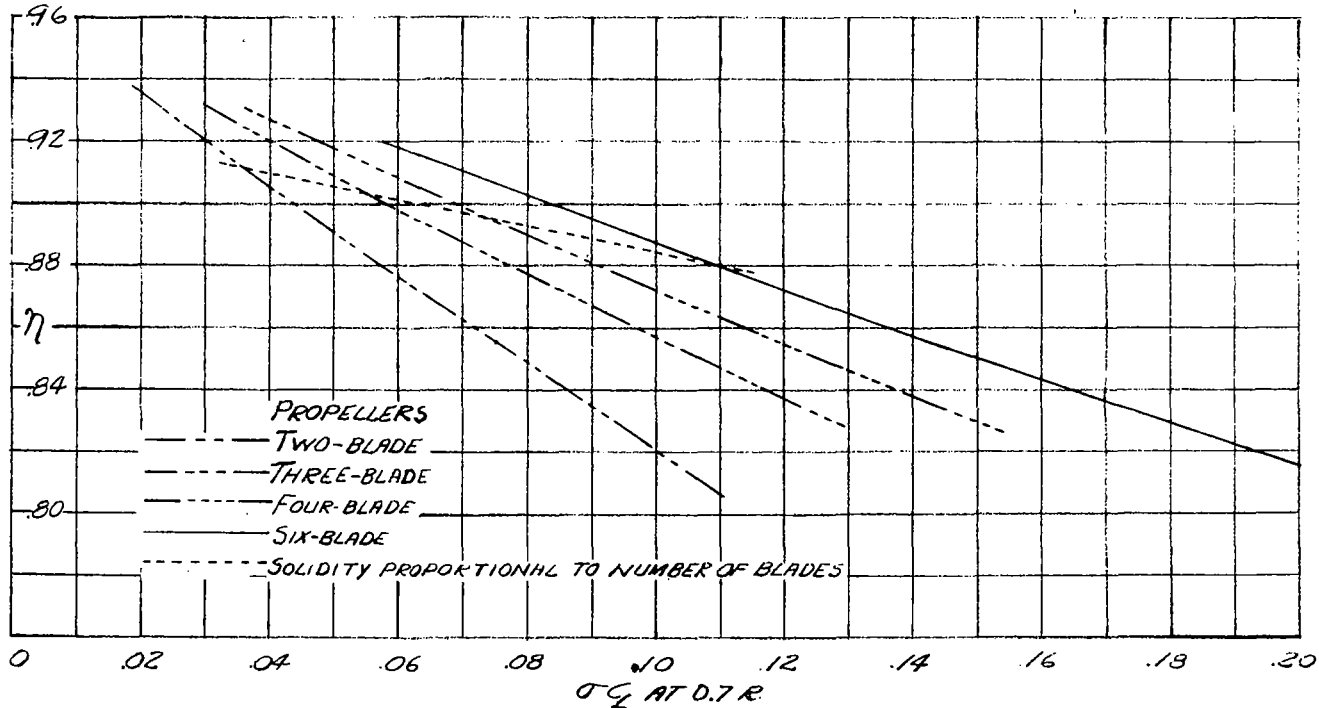

FIGURE 9.— OPTIMUM EFFICIENCY AGAINST σ_c AT 0.7 RADIUS FOR $V/nD = 2.5$. ELEMENT $4/D_0 = 60$.

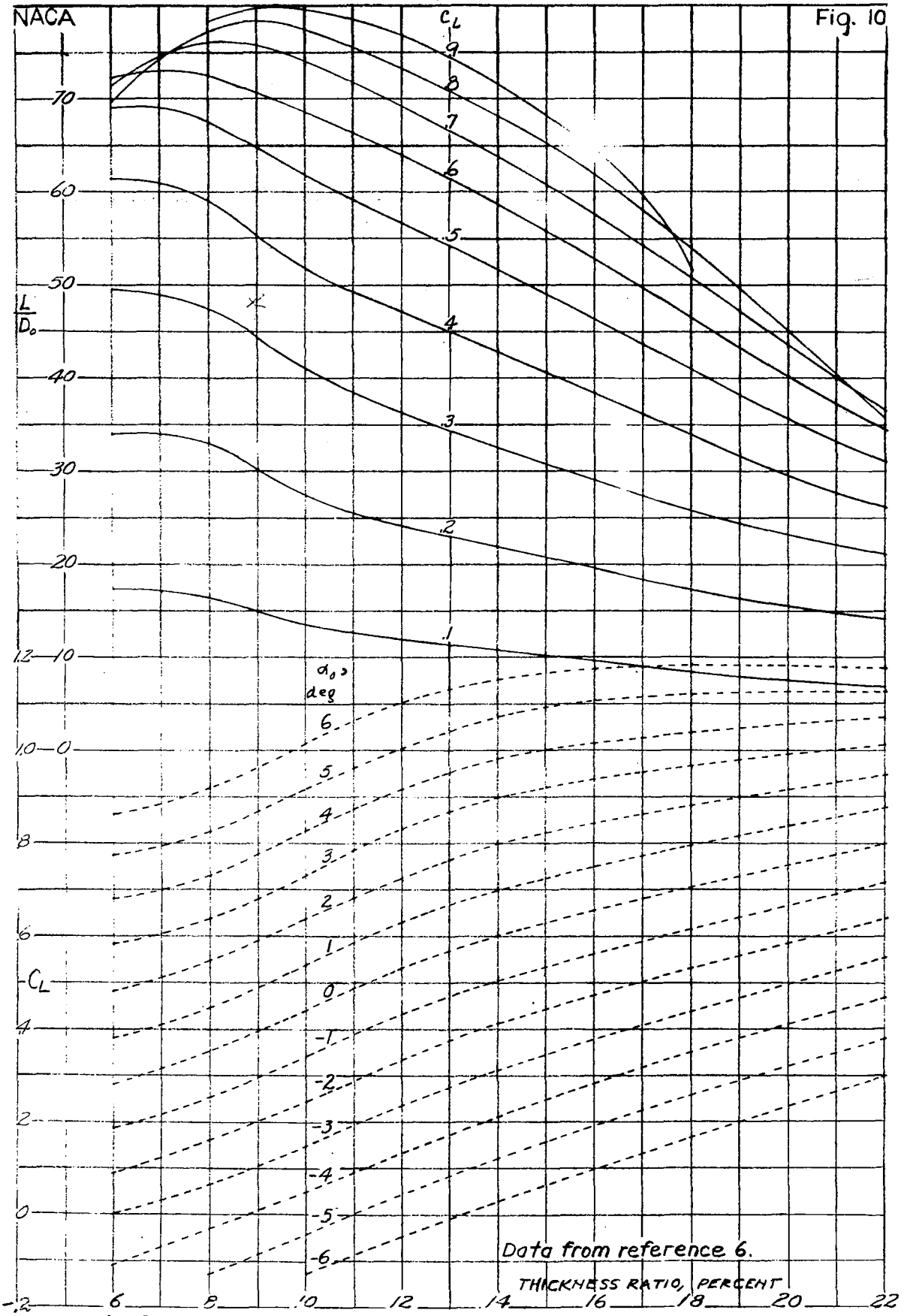

FIGURE 10.- CHARACTERISTICS OF CLARK Y AIRFOILS CORRECTED TO INFINITE ASPECT RATIO

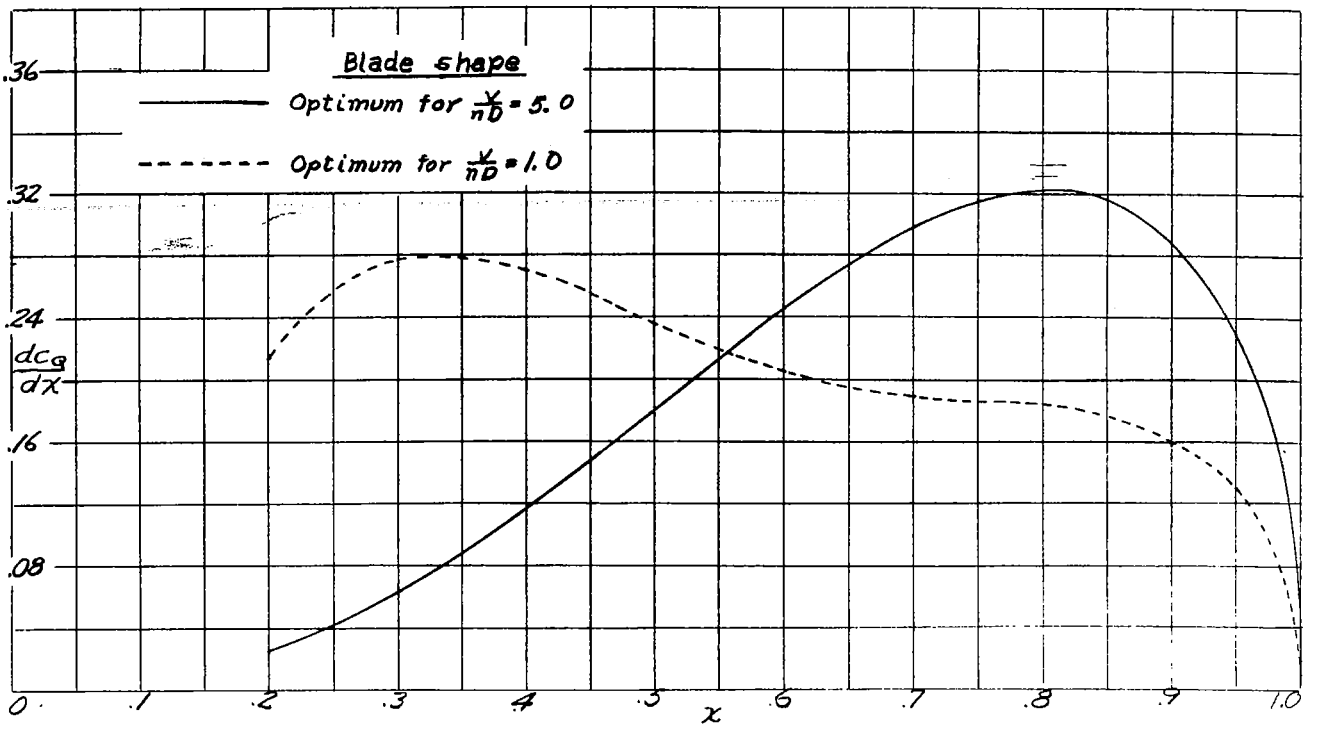

FIGURE 11.— COMPARISON OF TORQUE DISTRIBUTIONS FOR OPTIMUM PROPELLER AND FOR PROPELLER WITH BLADES TURNED IN HUB. B, 3; V/nD=5.0.

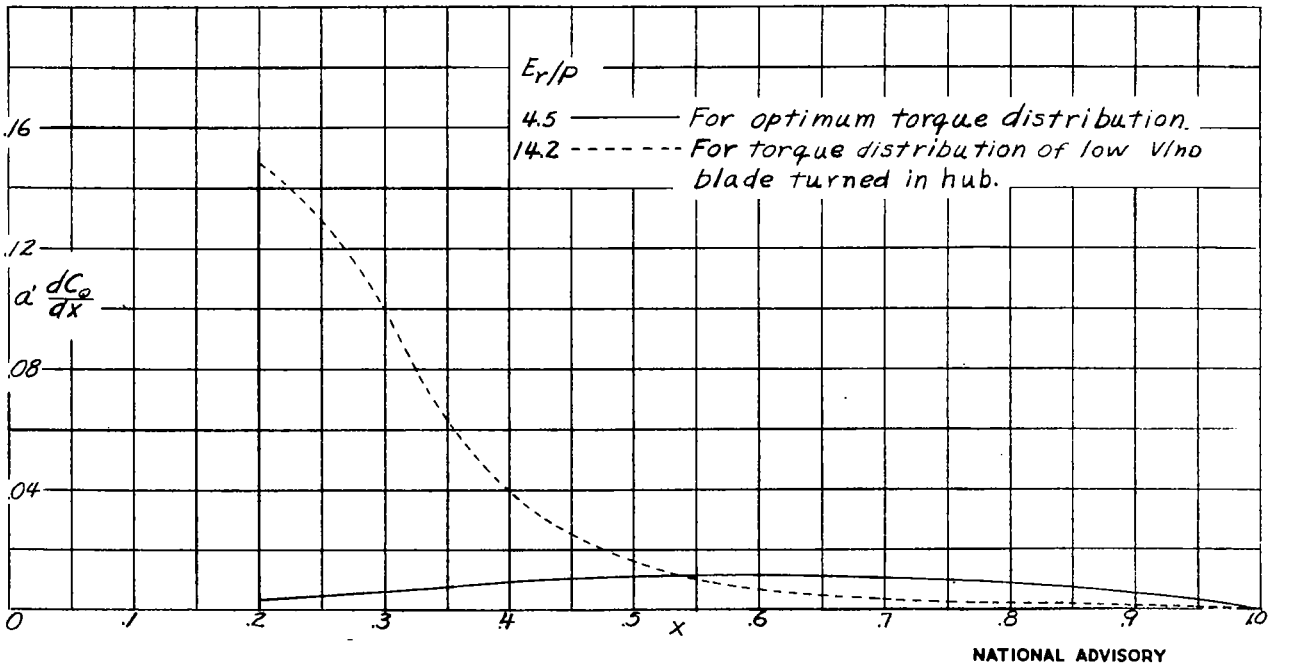

Figure 12.- Curves of $a' \frac{dC_Q}{dx}$ against x. V/nD = 5.0

NATIONAL ADVISORY COMMITTEE FOR AERONAUTICS